

tension) and due to the smaller area through which all the jet volume must flow, the velocity of the fluid below the free surface would accelerate rapidly. Associated with this acceleration would be a decrease in pressure and the resulting non-hydrostatic vertical pressure gradient would curve the streamlines downward at the jet exit. Keller's model (Keller 1957) shows that the pressure at the lip of the orifice about which the flow is attached goes to zero. His analysis was inviscid, but the magnitude of the downward force caused by the pressure at the lower lip being quite small is certain to be significant.

It should be noted that the mechanism of the teapot effect discussed above does not require surface tension. However, the role of surface tension in the experiments reported here will be one which determines when separation occurs within the jet channel. The contact line between the ambient jet and the vertical wall which is flush with the jet will be of greatest importance and is controlled by many factors including the surface tension of the host fluid. Changes in the dynamic contact angle are one possible explanation for the observed hysteresis in transition location.

The authors would like to acknowledge helpful discussions with Y. Jaluria and L. Scriven.

References

- Anwar, H. O. 1969: Behavior of buoyant jet in calm fluid. *J. Hydraulics Div., ASCE*, 95, 1289–1303
- Balasubramanian, V.; Jain, S. C. 1979: Horizontal buoyant jets in quiescent shallow water. *J. Environmental Div., ASCE*, 104, 717–729
- Chan, D. T. L.; Kennedy, J. F. 1975: Submerged buoyant jets in quiescent fluids. *J. Hydraulics Div., ASCE*, 101, 733–741
- Davis, L. R.; Shirazi, M. A.; Slegel, D. L. 1978: Measurement of buoyant jet entrainment from single and multiple sources. *J. Heat Transfer*, 100, 442–447
- Engelund, F.; Pedersen, F. B. 1973: Surface jet at small Richardson number. *J. Hydraulics Div., ASCE*, 99, 405–416
- Engelund, F. 1976: Hydraulics of surface buoyant jet. *J. Hydraulics Div., ASCE*, 102, 1315–1325
- Jen, Y.; Wiegel, R. L.; Mobarek, I. 1966: Surface discharge of horizontal warm-water jet. *J. Power Div., ASCE*, 92, 1–12
- Jirka, G. H.; Harleman, D. R. F. 1979: Stability and mixing of a vertical plane buoyant jet in confined depth. *J. Fluid Mech.*, 94, 275–304
- Karwe, M. 1983: An experimental study of the entrance location effects on buoyant surface jets. M. Sc. Diss. Rutgers University
- Keller, J. B. 1957: Teapot effect. *J. Applied Physics*, 28, 859–864
- Koh, R. C. Y. 1971: Two-dimensional surface warm jets. *J. Hydraulics Div., ASCE*, 97, 819–836
- Quraishi, M. S.; Fahidy, T. Z. 1982: A flow visualization technique using analytical indicators: Theory and some applications. *Chem. Eng. Sci.* 37, 775–780
- Reister, J. B.; Bajura, R. A.; Schwartz, S. H. 1980: Effects of water temperature and salt concentration on the characteristics of horizontal buoyant submerged jets. *J. Heat Transfer*, 102, 557–562
- Tamai, N.; Wiegel, R. L.; Tornberg, G. F. 1969: Horizontal surface discharge of warm water jets. *J. Power Div., ASCE*, 95, 253–276
- Wiuff, R. 1978: Experiments on surface buoyant jet. *J. Hydraulics Div., ASCE*, 104, 667–678

Received August 8, 1983

Technical notes

Optical measurement of profile and contact angle of liquids on transparent substrates

Y. Xu, N. Zhang, W.-J. Yang and C. M. Vest

Department of Mechanical Engineering and Applied Mechanics, University of Michigan, Ann Arbor, MI 48109, USA

1 Introduction

A simple method, based on holographic and shearing interferometry, has been developed and used to measure the profile of liquid droplets in equilibrium with air on flat, horizontal glass substrates. Apparent contact angles can be determined with relative ease. We have observed that some liquids have surface profiles with an inflection

near the contact line rather than monotonic profiles such as those generally assumed in theoretical work.

The detailed profile of the liquid-vapor (or gas) interface near the contact line is important for determining wetting characteristics, apparent contact angle, and solid-liquid surface tension. Usually the Young-Dupre equation is used to calculate the profile of the liquid-vapor interface near the line of contact with a solid. Recently the Young-

Laplace equation of capillarity, augmented by the disjoining pressure concept of Deryagin has been used to obtain these profiles for systems with finite contact angles by Wayner (1980). Contact angles in free films also have been studied using this equation by Wayner (1980), DeFeijter et al. (1978), Wayner (1982) and Ivanov and Toshev (1975). Wayner (1982) demonstrated that the Young-Dupre equation is a modified and simplified version of the Young-Laplace equation. Both equations result from the application of continuum concepts at the molecular level and neglect gravitational effects.

Because these theoretical approaches to calculating profiles are restricted to regions very near the contact line and neglect effects such as gravity and evaporation, an experimental approach is desirable. In this paper, we report the first experiments in which an accurate optical technique has been used to visualize and measure the profiles of entire liquid drops on solid substrates.

2 Principle

The droplet of liquid under study is placed on a transparent substrate which in turn is placed on the emulsion of a high-resolution photographic plate. The droplet is then illuminated from above by two plane waves of laser light which propagate with an angle 2θ between them and which are oriented symmetrically about the normal to the plate as shown in Fig. 1. Two sequential exposures of the plate are made – one before the drop is placed on the substrate and one after it is so placed. After this plate is developed it contains two superimposed, high spatial frequency, grating-like interference fringe patterns. One of these gratings consists of parallel, straight, equally-spaced fringes. The other grating is distorted because of the optical effects of the droplet. A set of moiré fringes indicative of the difference of these two gratings can be observed over most of the droplet cross-section by illuminating the developed plate with ordinary white light.

Figure 2 is a schematic diagram showing various optical rays passing through the droplet and substrate.

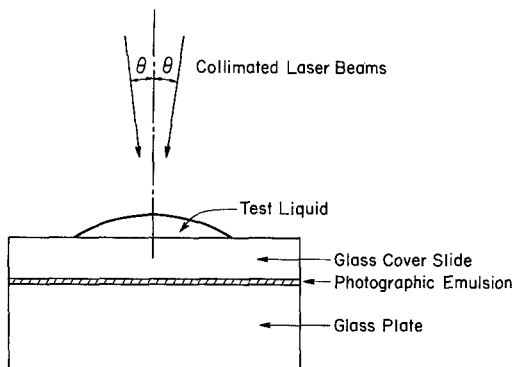


Fig. 1. Schematic diagram of test apparatus

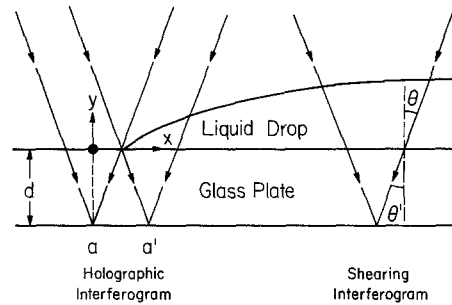


Fig. 2. Typical optical rays in the two domains: holographic interferometry and shearing interferometry

Two types of fringes occur. Those fringes which appear in the peripheral region $a-a'$ form a holographic interferogram which can be observed by illuminating the photographic plate with white light travelling in the same direction as the left-most ray shown in Fig. 2. The profile in this narrow peripheral region can approximately be determined using the relation

$$y \cong N\lambda/[n \cos(\theta') - \cos(\theta)] \quad (1)$$

where

$$\cos(\theta') = \sqrt{1 - [\sin(\theta)/n]^2} \quad (2)$$

The refractive index of the liquid n is defined as $\sin \theta / \sin \theta'$. In Eqs. (1) and (2) y is the height of the liquid surface, λ is the wavelength of laser light and N is the fringe order number which is assigned integer values at the center of each bright fringe sequentially from the outer edge of the droplet. This analysis is approximate because it is developed under the assumption that the slope of the surface is very small, θ is small, and the refractive index of the liquid, n , is nearly equal to the refractive index of the substrate. However, these approximations are quite reasonable for the particular liquid-glass systems discussed in this note. A more detailed iterative computation can be performed to obtain accurate profiles in the general case.

The second set of fringes, which generally appears over most of the liquid cross-section, constitutes a shearing interferogram. An approximate analysis of the liquid profile can be made using Eq. (3):

$$dy/dx \cong N\lambda/\{2(y+d)[n \cos(\theta') - \cos(\theta)] \tan(\theta')\} \quad (3)$$

Here, d denotes the glass plate thickness and x is the coordinate defined in Fig. 2. A more accurate determination of liquid surface profile can be obtained by an iterative ray tracing procedure using the results of Eq. (3) as an initial approximation.

3 Results

In the present experiments the liquid samples were deposited by using a monojet microsyringe in $8 \mu\text{l}$ drops onto

clean glass cover slides. The cover slides were placed on plates of Agfa-Gaevert 8E75 holographic plates which were exposed to He-Ne laser beams as described above. Figure 3 is a photograph of the fringe pattern obtained using cyclohexane ($n=1.44507$) as the test fluid. As indicated in Fig. 4, the closed fringes in the outer region of the drop indicate that there is a reversal of curvature. Such reversals have been theorized to occur in microlayers near the periphery of liquids in contact with certain solids. In this experiment the reversal occurs where the droplet height is $21\ \mu\text{m}$. This effect was observed with 100 percent repeatability during several tests with this liquid.

Interferograms were obtained in the same way using a light oil which had a refractive index nearly matching that of glass as the test fluid. When these interferograms are

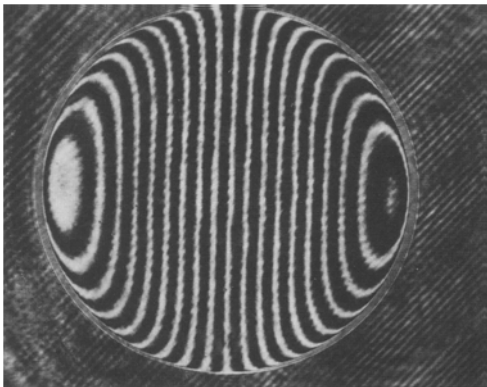


Fig. 3. Fringe system for droplet of cyclohexane on glass

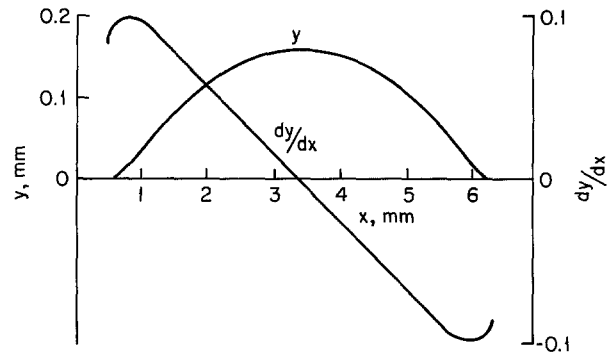


Fig. 4. Droplet profile and slope determined using the interferogram in Fig. 3

examined under a microscope, reversal of curvature can be observed very near the contact line.

References

- Wayner, P. C., Jr., 1980: Interfacial profile in the contact line region of a finite contact angle system. *J. Colloid Interface Sci.* 77, 495–500
- DeFeijter, J. A.; Rijnbout, J. B., Vrij, J. 1978: Contact angles in thin liquid films. *J. Colloid Interface Sci.* 64, 258–277
- Ivanov, I. B.; Toshev, B. V. 1975: Thermodynamics of thin liquid films, *Colloid Polym. Sci.* 253, 593–599
- Wayner, P. C., Jr. 1982: The interfacial profile in the contact line region and the Young-Dupre equation. *J. Colloid Interface Sci.* 88, 294–295

Received January 23, 1984